Journal of Physics and Advanced Applications
Volume 1 | Issue 1

HELICS GROUP LLC
Scientific Networks

Research Article Open Access

Dust Acoustic Shock Waves in a Six Component Charge Varying Cometary Plasma

Neethu TW[1], Shilpa S[2], Philip NS[3] and Venugopal C[4*]

[1]Department of Physics, CMS College, Kottayam - 686001, Kerala, India.
[2]International School of Photonics, Cochin University of Science and Technology, Kochi-682022, Kerala, India.
[3]Artificial Intelligence Research and Intelligent Systems, Thelliyoor – 689544, Kerala, India.
[4]School of Pure and Applied Physics, Mahatma Gandhi University, Kottayam, Kerala, India.

***Corresponding author:** Venugopal Chandu, School of Pure and Applied Physics, Mahatma Gandhi University, Kottayam, Kerala, India, E-mail: cvgmgphys@yahoo.co.in*

Citation: Venugopal C, Neethu TW, et al. (2020) Dust Acoustic Shock Waves in a Six Component Charge Varying Cometary Plasma. J Phy Adv App 1(1): 1-12.

Received Date: June 01, 2020; **Accepted Date:** June 07, 2020; **Published Date:** June 09, 2020

Abstract

Dust acoustic shock waves have been studied in six component cometary plasma by deriving the Korteweg-deVries-Burgers (KdVB) equation. The constituents of the plasma include two components of electrons described by kappa distributions with different temperatures and spectral indices, lighter (hydrogen) ions and a pair of oppositely charged, heavier ions (positively and negatively charged oxygen ions), all of them described by Maxwellian distributions with different temperatures. Charge varying negatively charged dust grains is the sixth component.

Shock waves solutions of the KdVB equation, studied for typical parameters of comet Halley, show that the shock amplitudes are consistently larger when charge fluctuations on the dust grains are taken into consideration. The superthermal, second component of electrons affects the phase velocity and the shock velocity as well as it's width. The amplitude of the shock wave is also affected by the densities and temperatures of all the ions: it increases with increasing positively charged oxygen ion densities and decreases with increasing temperatures of these ions. The amplitude, however, decreases with increasing densities and increases with increasing temperatures of the other two types of ions.

Key Words: Cometary plasma; Shock waves; Dusty plasma; Charge variation; 6 components;

Introduction

The presence of charged dust grains introduces new features to the non-linear structures in space environments such as planetary rings, planetary magnetospheres, comet environments, interstellar media and earth-space environments [1-4]. The non-linearities in dusty plasmas give rise to localization of waves, generating different types of fascinating coherent structures, namely, solitary structures [5], double layers [6], shock waves [7], vortices [8,9] etc. In dusty plasmas, the interaction of dust grains with energetic particles such as electrons and ions lead to the charging of dust grains. The charging currents to the dust grains carried by the plasma particles can be calculated using the Orbital Motion Limited (OML) approach [10,11]. Extensive studies on the effect of dust charge variation on solitary [12-15] and shock structures [16-18] have been carried out.

There is a strong current interest to understand the relevance of the dust charge variation on the formation of dust acoustic shock waves [19-21]. Popel et al [22] discussed the possibility of the observation of shock waves related to the dust charging process in the presence of electromagnetic radiation in active rocket experiments which involved the release of some gaseous substances in the near-earth space. Further, Duha et al [23] investigated the dust-ion-acoustic solitary and shock waves associated with the dynamics of negative ions, Maxwellian positive ions, trapped electrons and charge fluctuating stationary dust by employing the reductive perturbation method. Several authors [24-26] have

studied Dust-Acoustic (DA) shock waves in a charge varying non-extensive dusty plasma. Hadjaz and Tribeche [27] obtained a dusty plasma model that supported solitary as well as shock waves, for which the main properties such as phase velocity, amplitude and width were drastically influenced by trapping, nonthermality and charge variation. El-Shewy et al [28] highlighted the effects of dust viscosity and electron-ion nonthermality fraction on DA shock waves in inhomogeneous dusty plasmas with nonadiabatic dust charge fluctuation. Later, Wang et al [29] studied the effects of dust size distribution and dust charge fluctuation of dust grains on small but finite amplitude nonlinear dust ion-acoustic shock waves, in an unmagnetized multi-ion dusty plasma.

In a large number of space environments, velocity distributions have commonly been reported that are Maxwellian-like in the low-energy range, but possesses a power-law tail at superthermal particle energies [30-34]. Such distributions are modeled by a generalized form of Lorentzian or kappa distribution first proposed by Vasyliunas [35]. The Maxwellian distribution is a special case of the kappa function; in the limit of the spectral index $\kappa \to \infty$. In a recent study, Broiles et al [36] evaluated the observations made by Rosetta spacecraft of the superthermal electron environments near comet 67P/Churyumov-Gerosimenko and fitted the observed electron velocity space densities with a combination of two three-dimensional kappa distributions. Hence there has been a great deal of interest in studies related to dust charge fluctuation on shock waves in a suprathermal dusty plasma [37-39]. Recently, Ferdousi et al [40] analysed the properties of low frequency dust-acoustic shock waves in a plasma medium in the presence of superthermal kappa distributed electrons.

A cometary plasma has been observed to be a genuine multi-ion plasma as it is composed of solar wind protons and electrons;the dissociation of water molecules contributes positively charged hydrogen (H^+) and oxygen (O^+) and photo-electrons [41]. In addition to the existence of positive ions, negative ions have also been observed in cometary plasmas [42]. Besides, the above mentioned ion pairs, dust of opposite polarities has also been observed in cometary environments [43,44]. Hence, Manesh et al [45] investigated the existence of Ion-Acoustic (IA) shock waves in a five component cometary plasma consisting of positively and negatively charged oxygen ions, kappa described hydrogen ions, hot solar electrons, and slightly colder cometary electrons. Very recently, Sijo et al [46] studied the effect of the drift velocity of lighter ions on shock waves in the above five component cometary plasma. Further, Mahmoud [47] analyzed the effects of the non-extensive parameters on the structure of the envelope ion acoustic waves in five-component cometary plasma system containing positively and negatively charged oxygen ions, non-extensive hot electrons from solar origin, colder electrons of cometary origin and positive hydrogen ions.

Thus for reasons given above, we investigate the effect of dust charge variation on dust acoustic shock waves in a six component cometary plasma composed of lighter hydrogen ions, positively and negatively charged oxygen ions, charge varying dust grains of negative polarity, cometary photo-electrons and hot, solar wind electrons.

Basic Equations

We consider a six component, unmagnetized plasma containing negatively charged dust (denoted by subscript 'd'), negatively and positively charged oxygen ions (denoted by subscripts '**1**' and '**2** ' respectively), positive hydrogen ions (denoted by subscript 'H') and superthermal electrons described by kappa distributions (hot electrons from solar origin and colder electrons of cometary origin denoted by subscripts 'he' and 'ce', respectively).

At equilibrium, charge neutrality requires:

$$n_{ce0} + n_{he0} + z_{10}n_{10} + z_{d0}n_{d0} = n_{H0} + z_{20}n_{20} \quad (1)$$

where n_{he0} and n_{ce0} represent the equilibrium densities of cometary electrons and solar electrons respectively; n_{10}, n_{20}, n_{H0} and n_{d0} are the equilibrium densities of negatively charged oxygen (O^-) ions, positively charged oxygen (O^+) ions, hydrogen ions and negatively charged dust respectively. z_{10}, z_{20} and z_{d0} are the equilibrium charge numbers of O^-, O^+ ions and dust respectively.

The dynamics of the negatively charged dust particles can be described by the following hydrodynamic equations:

$$\frac{\partial n_d}{\partial t} + \frac{\partial (n_d v_d)}{\partial x} = 0 \quad (2)$$

$$\frac{\partial v_d}{\partial t} + v_d \frac{\partial v_d}{\partial x} = \frac{z_d e}{m_d}\frac{\partial \phi}{\partial x} + \eta_d \frac{\partial^2 v_d}{\partial x^2} \quad (3)$$

$$\frac{\partial^2 \phi}{\partial x^2} = 4\pi e \left[n_{ce} + n_{he} + z_{10}n_1 + z_d n_d - n_H - z_{20}n_2 \right] \quad (4)$$

where v_d and $\eta_d$are the fluid velocity and kinematic viscosity of the dust grains,m_d, the mass and e, the electronic charge.

The above equations, in their dimensionless forms, are:

$$\frac{\partial n_d}{\partial t} + \frac{\partial (n_d v_d)}{\partial x} = 0 \quad (5)$$

$$\frac{\partial v_d}{\partial t} + v_d \frac{\partial v_d}{\partial x} = z_d \frac{\partial \phi}{\partial x} + \eta_d \frac{\partial^2 v_d}{\partial x^2} \quad (6)$$

$$\frac{\partial^2\phi}{\partial x^2} = z_d n_d + \delta_{ce}\left[1-\frac{s\beta_H\phi}{\left(\kappa_{ce}-\frac{3}{2}\right)}\right]^{-\kappa_{ce}+\frac{1}{2}} + \delta_{he}\left[1-\frac{s\beta_{H3}\phi}{\left(\kappa_{he}-\frac{3}{2}\right)}\right]^{-\kappa_{he}+\frac{1}{2}}$$

$$+\delta_1\exp\left(s\beta_{H1}\phi\right)-\delta_H\exp\left(-s\phi\right)-\delta_2\exp\left(-s\beta_{H2}\phi\right) \quad (7)$$

where the kappa distributions model the number densities for cometary (ce) and solar (he) electrons; while the hydrogen ions (denoted by H, negatively charged oxygen ions (identified by '1') and positively charged oxygen ions ('2') obey a Maxwellian distribution. The dust grain density is normalized by n_{d0} and z_d by z_{d0}; the densities of electrons and ions are normalized by $z_{d0}n_{d0}$. The space $'x'$ and $'t'$ time coordinates are normalized by the Debye length $\lambda_{Dd}=[\frac{Teff}{4\pi z_{d0}n_{d0}e^2}]^{\frac{1}{2}}$ and the inverse of dust plasma frequency $\omega_{pd}^{-1}=[\frac{4\pi z_{d0}^2e^2n_{d0}}{m_d}]^{\frac{-1}{2}}$ respectively. The dust fluid velocity v_d and electostatic potential are normalized by the DA speed $C_d=[\frac{z_{d0}T_{eff}}{m_d}]^{\frac{1}{2}}$ and $\frac{T_{eff}}{e}$, respectively, in which the effective temperature T_{eff} is [48]:

$$T_{eff}=\frac{z_{d0}n_{d0}}{\left[\frac{n_{he0}}{T_{he}}+\frac{n_{ce0}}{T_{ce}}+\frac{z_{10}n_{10}}{T_1}+\frac{z_{20}n_{20}}{T_2}+\frac{n_{H0}}{T_H}\right]} \quad (8)$$

Also $\delta_H=\frac{n_{H0}}{z_{d0}n_{d0}}$, $\delta_1=\frac{z_{10}n_{10}}{z_{d0}n_{d0}}$, $\delta_2=\frac{z_{20}n_{20}}{z_{d0}n_{d0}}$, $\delta_{ce}=\frac{n_{ce0}}{z_{d0}n_{d0}}$, $\delta_{he}=\frac{n_{he0}}{z_{d0}n_{d0}}$, $\beta_H=\frac{T_H}{T_{ce}}$, $\beta_1=\frac{T_1}{T_{ce}}$ $\beta_2=\frac{T_2}{T_{ce}}$, $\beta_{he}=\frac{T_{he}}{T_{ce}}$, $\beta_{H1}=\frac{\beta_H}{\beta_1}=\frac{T_H}{T_1}$, $\beta_{H2}=\frac{\beta_H}{\beta_2}=\frac{T_H}{T_2}$, $\beta_{H3}=\frac{\beta_H}{\beta_{he}}=\frac{T_H}{T_{he}}$, $s=\frac{T_{eff}}{T_H}=\frac{\delta_H-\delta_1+\delta_2-\delta_{ce}-\delta_{he}}{\delta_H+\delta_1\beta_{H1}+\delta_2\beta_{H2}+\delta_{ce}\beta_H+\delta_{he}\beta_{H3}}$

where T_d, T_{ce}, T_{he}, T_H, T_1 and T_2 are the temperatures of dust, cometary electrons, solar electrons, hydrogen ions, negative and positive oxygen ions, respectively.

The variable dust charge z_d is obtained from the current balance equation,

$$I_H+I_1+I_2+I_{ce}+I_{he}=0 \quad (9)$$

where I_H, I_1, I_2, I_{ce} and I_{he} are hydrogen ion, negatively charged oxygen, positively charged oxygen, colder and hotter electron currents, respectively.

The ion currents are [11]:

$$I_H=e\pi r^2\left(\frac{8T_H}{\pi m_H}\right)^{\frac{1}{2}}n_H\left(1-\frac{e\phi_d}{T_H}\right) \quad (10)$$

$$I_2=z_2e\pi r^2\left(\frac{8T_2}{\pi m_2}\right)^{\frac{1}{2}}n_2\left(1-\frac{z_2e\phi_d}{T_2}\right) \quad (11)$$

where I_H and I_2 are the charging currents for attractive potentials ($q_j\phi_d<0$) due to hydrogen and positively charged oxygen ions respectively. Here ϕ_d denotes the dust grain surface potential relative to the plasma potential ϕ; r is the radius of the dust grain and the other notations are standard. Also

$$I_1=-z_1e\pi r^2\left(\frac{8T_1}{\pi m_1}\right)^{\frac{1}{2}}n_1\exp\left(\frac{z_1e\phi_d}{T_1}\right) \quad (12)$$

where I_1 is the charging current for a repulsive potential ($q_j\phi_d>0$) due to the negatively charged oxygen ions.

The currents due to the cometary and solar, kappa distributed electrons to the negatively charged dust grains are [49],

$$I_{ce}=-2\sqrt{\pi}r^2B_{\kappa_{ce}}en_{ce}\theta_{ce}\left(1-\frac{2e\phi_d}{\kappa_{ce}m_{ce}\theta_{ce}^2}\right)^{-\kappa_{ce}+1} \quad (13)$$

$$I_{he}=-2\sqrt{\pi}r^2B_{\kappa_{he}}en_{he}\theta_{he}\left(1-\frac{2e\phi_d}{\kappa_{he}m_{he}\theta_{he}^2}\right)^{-\kappa_{he}+1} \quad (14)$$

where $B_{\kappa j}=\left\{\frac{\Gamma\left(\kappa_j+1\right)}{\kappa_j^{3/2}\Gamma\left(\kappa_j-1/2\right)}\right\}\frac{\kappa_j}{\kappa_j-1}$ and θ, the effective thermal speed for the electron, is $\theta_j^2=\left(\frac{2\kappa_j-3}{\kappa_j}\right)\frac{T_j}{m_j}$; $j=ce,he$. Here m_j is the mass, n_j is the electron number density, T_j is the temperature and κ_j, the spectral index of the j^{th} species.

Using equations (10) - (14) in the current balance equation (9), we arrive at

$$b_H\delta_H\left(1-s\psi\right)e^{-s\phi}+b_2\delta_2\left(1-\beta_{H2}s\psi\right)e^{-\beta_{H2}s\phi}-b_1\delta_1e^{s\beta_{H1}\psi}e^{s\beta_{H1}\phi}-b_{\kappa_{ce}}\delta_{ce}\left(1-\frac{2\beta_Hs\psi}{\left(2\kappa_{ce}-3\right)}\right)^{-\kappa_{ce}+1}$$

$$\times\left[1-\frac{\beta_Hs\phi}{\left(\kappa_{ce}-\frac{3}{2}\right)}\right]^{-\kappa_{ce}+\frac{1}{2}}-b_{\kappa_{he}}b_3\delta_{he}\left(1-\frac{2\beta_{H3}s\psi}{\left(2\kappa_{he}-3\right)}\right)^{-\kappa_{he}+1}\left[1-\frac{\beta_{H3}s\phi}{\left(\kappa_{he}-\frac{3}{2}\right)}\right]^{-\kappa_{he}+\frac{1}{2}}=0 \quad (15)$$

where $b_H=\sqrt{\frac{2\beta_H}{\mu_H}}$, $b_1=\sqrt{\frac{2\beta_1}{\mu_1}}$, $b_2=\sqrt{\frac{2\beta_2}{\mu_2}}$, $b_3=\sqrt{\frac{\beta_{he}}{\mu_3}}$

$,b_{\kappa_{ce}}=B_{\kappa_{ce}}\sqrt{\frac{(2\kappa_{ce}-3)}{\kappa_{ce}}},b_{\kappa_{he}}=B_{\kappa_{he}}\sqrt{\frac{(2\kappa_{he}-3)}{\kappa_{he}}},\psi=\frac{e\phi_d}{T_{eff}},\quad \mu_H=\frac{m_H}{m_{ce}},$

$\mu_1=\frac{m_1}{m_{ce}}$, $\mu_2=\frac{m_2}{m_{ce}}$ and $\mu_3=\frac{m_{he}}{m_{ce}}=1$.

The number of charges residing on the dust grains, z_d, defined as $z_d=\frac{\psi}{\psi_0}$ [50]; where $\psi_0=\psi(\phi=0)$ is the dust surface is floating potential corresponding to the unperturbed plasma potential and is determined from the following expression,

$$b_H\delta_H(1-s\psi_0)+b_2\delta_2(1-\beta_{H2}s\psi_0)-b_1\delta_1e^{s\beta_{H1}\psi_0}-b_{\kappa_{ce}}\delta_{ce}\left(1-\frac{2\beta_H s\psi_0}{(2\kappa_{ce}-3)}\right)^{-\kappa_{ce}+1}$$

$$-b_{\kappa_{he}}b_3\delta_{he}\left(1-\frac{2\beta_{H3}s\psi_0}{(2\kappa_{he}-3)}\right)^{-\kappa_{he}+1}=0 \qquad (16)$$

z_d can be expanded in terms of ϕ as follows

$$z_d=1+\gamma_1\phi+\gamma_2\phi^2+\cdots \qquad (17)$$

where $\gamma_1=\frac{\psi_0^{'}}{\psi_0}$ and $\gamma_2=\frac{\psi_0^{''}}{2\psi_0}$ come from expanding ψ near ψ_0.

Taking the derivative of equation (15) with respect to ϕ and finding its value at $\phi=0$ gives,

$$\psi_0^{'}=\frac{\gamma_b}{\gamma_a}$$

and hence,

$$\gamma_1=\frac{\gamma_b}{\psi_0\gamma_a}$$

of which,

$$\gamma_a=b_H\delta_H+b_2\delta_2\beta_{H2}+b_1\delta_1\beta_{H1}e^{s\beta_{H1}\psi_0}$$

$$+\frac{b_{\kappa_{ce}}\delta_{ce}\beta_H(\kappa_{ce}-1)}{\left(\kappa_{ce}-\frac{3}{2}\right)}\left(1-\frac{2\beta_H s\psi_0}{(2\kappa_{ce}-3)}\right)^{-\kappa_{ce}}+\frac{b_{\kappa_{he}}b_3\delta_{he}\beta_{H3}(\kappa_{he}-1)}{\left(\kappa_{he}-\frac{3}{2}\right)}\left(1-\frac{2\beta_{H3}s\psi_0}{(2\kappa_{he}-3)}\right)^{-\kappa_{he}}, \qquad (18)$$

$$\gamma_b=-b_H\delta_H(1-s\psi_0)-b_1\delta_1\beta_{H1}e^{\beta_{H1}s\psi_0}-b_2\delta_2\beta_{H2}(1-\beta_{H2}s\psi_0)$$

$$-\frac{b_{\kappa_{ce}}\delta_{ce}\beta_H\left(\kappa_{ce}-\frac{1}{2}\right)}{\left(\kappa_{ce}-\frac{3}{2}\right)}\left(1-\frac{2\beta_H s\psi_0}{(2\kappa_{ce}-3)}\right)^{-\kappa_{ce}+1}-\frac{b_{\kappa_{he}}b_3\delta_{he}\beta_{H3}\left(\kappa_{he}-\frac{1}{2}\right)}{\left(\kappa_{he}-\frac{3}{2}\right)}\left(1-\frac{2\beta_{H3}s\psi_0}{(2\kappa_{he}-3)}\right)^{-\kappa_{he}+1} \qquad (19)$$

Taking the second derivative of (15), with respect to ϕ, and finding its value at $\phi=0$ further gives,

$$\gamma_2=\frac{\psi_0^{''}}{2\psi_0}$$

And, therefore, $\gamma_2=\frac{\gamma_c}{2\psi_0\gamma_a}$.

where

$$\gamma_c=\gamma_{c1}+\gamma_{c2}+\gamma_{c3}$$

with

$$\gamma_{c1}=s\left[\begin{array}{l} b_H\delta_H(1-s\psi_0)+b_2\delta_2\beta_{H2}^2(1-\beta_{H2}s\psi_0)-b_1\delta_1\beta_{H1}^2e^{s\beta_{H1}\psi_0}-\frac{b_{\kappa_{ce}}\delta_{ce}\beta_H^2\left(\kappa_{ce}^2-\frac{1}{4}\right)}{(\kappa_{ce}-\frac{3}{2})^2}\times \\ \times\left(1-\frac{2\beta_H s\psi_0}{(2\kappa_{ce}-3)}\right)^{-\kappa_{ce}+1}-\frac{b_{\kappa_{he}}b_3\delta_{he}\beta_{H3}^2\left(\kappa_{he}^2-\frac{1}{4}\right)}{(\kappa_{he}-\frac{3}{2})^2}\left(1-\frac{2\beta_{H3}s\psi_0}{(2\kappa_{he}-3)}\right)^{-\kappa_{he}+1} \end{array}\right] \qquad (20)$$

$$\gamma_{c2}=2s(\gamma_1\psi_0)\left[b_H\delta_H+b_2\delta_2\beta_{H2}^2-b_1\delta_1\beta_{H1}^2e^{s\beta_{H1}\psi_0}-\frac{b_{\kappa_{ce}}\delta_{ce}\beta_H^2(\kappa_{ce}-1)\left(\kappa_{ce}-\frac{1}{2}\right)}{(\kappa_{ce}-\frac{3}{2})^2}\right.$$

$$\left.\times\left(1-\frac{2\beta_H s\psi_0}{(2\kappa_{ce}-3)}\right)^{-\kappa_{ce}}-\frac{b_{\kappa_{he}}b_3\delta_{he}\beta_{H3}^2(\kappa_{he}-1)\left(\kappa_{he}-\frac{1}{2}\right)}{(\kappa_{he}-\frac{3}{2})^2}\left(1-\frac{2\beta_{H3}s\psi_0}{(2\kappa_{he}-3)}\right)^{-\kappa_{he}}\right. \qquad (21)$$

and

$$\gamma_{c3}=-s(\gamma_1\psi_0)^2\left[b_1\delta_1\beta_{H1}^2e^{s\beta_{H1}\psi_0}+\frac{b_{\kappa_{ce}}\delta_{ce}\beta_H^2\kappa_{ce}(\kappa_{ce}-1)}{(\kappa_{ce}-\frac{3}{2})^2}\left(1-\frac{2\beta_H s\psi_0}{(2\kappa_{ce}-3)}\right)^{-\kappa_{ce}-1}\right.$$

$$\left.+\frac{b_{\kappa_{he}}b_3\delta_{he}\beta_{H3}^2\kappa_{he}(\kappa_{he}-1)}{(\kappa_{he}-\frac{3}{2})^2}\left(1-\frac{2\beta_{H3}s\psi_0}{(2\kappa_{he}-3)}\right)^{-\kappa_{he}-1}\right. \qquad (22)$$

Dust acoustic shock waves - Derivation of KdVB equation:

We shall derive the KdVB equation by employing the reductive perturbation method [51]. The stretched co-ordinates are introduced in the following form [50],

$$\xi=\epsilon^{\frac{1}{2}}(x-\lambda t),$$

$$\tau=\epsilon^{\frac{3}{2}}t$$

$$\eta_d=\epsilon^{\frac{1}{2}}\eta_{d0} \qquad (23)$$

where ϵ is a small parameter that measures the size of the perturbation amplitude and λ is the velocity of the shock wave normalized by C_d. In a weak damping situation, the kinematic viscosity of dust ions can be considered small but finite. Here, η_{d0} is a finite parameter.

The various parameters are expanded as a power series in ϵ as

$$n_d = 1 + \in n_d^{(1)} + \in^2 n_d^{(2)} + \cdots \quad (24)$$

$$v_d = \in v_d^{(1)} + \in^2 v_d^{(2)} + \cdots \quad (25)$$

$$\phi = \in \phi^{(1)} + \in^2 \phi^{(2)} + \cdots \quad (26)$$

Also from equation (17),

$$z_d = 1 + \in \left(\gamma_1 \phi^{(1)}\right) + \in^2 \left(\gamma_1 \phi^{(2)} + \gamma_2 \left[\phi^{(1)}\right]^2\right) + \cdots \quad (27)$$

Using transformation equations in equations (5)-(7) and equating different powers of $\in$, the lowest order of $\in$ leads to:

$$n_d^{(1)} = \frac{-\phi^{(1)}}{\lambda^2}$$

$$v_d^{(1)} = \frac{-\phi^{(1)}}{\lambda} \quad (28)$$

Equating terms of power of order ϵ in Poisson's equation, the linear dispersion relation of the wave can be expressed as:

$$\left[\gamma_1 + s\left(\delta_H + \delta_1\beta_{H1} + \delta_2\beta_{H2} + \frac{\delta_{he}\left(\kappa_{he} - \frac{1}{2}\right)\beta_{H3}}{\left(\kappa_{he} - \frac{3}{2}\right)} + \frac{\delta_{ce}\left(\kappa_{ce} - \frac{1}{2}\right)\beta_H}{\left(\kappa_{ce} - \frac{3}{2}\right)}\right)\right]\lambda^2 = 1 \quad (29)$$

Next, equating terms of order in $\in^{\frac{5}{2}}$ and using equations (28), we get:

$$\frac{\partial n_d^{(2)}}{\partial \xi} = -\frac{2}{\lambda^3}\frac{\partial \phi^{(1)}}{\partial \tau} + \left[\frac{3}{\lambda^4} - \frac{\gamma_1}{\lambda^2}\right]\phi^{(1)}\frac{\partial \phi^{(1)}}{\partial \xi} - \frac{1}{\lambda^2}\frac{\partial \phi^{(2)}}{\partial \xi} + \frac{\eta_{d0}}{\lambda^3}\frac{\partial^2 \phi^{(1)}}{\partial \xi^2} \quad (30)$$

Simiarly, equating coefficients of terms of order $\in^2$ from Poisson's equation, we get

$$\frac{\partial^2 \phi^{(1)}}{\partial \xi^2} = n_d^{(2)} + \gamma_1 \phi^{1)} n_d^{(1)} + \gamma_2 [\phi^{(1)}]^2 + P\phi^{(2)} + Q\frac{[\phi^{(1)}]^2}{2} \quad (31)$$

where

$$P = \left[\gamma_1 + s\delta_H + s\delta_1\beta_{H1} + s\delta_2\beta_{H2} + s\delta_{he}\beta_{H3}\frac{\left(\kappa_{he} - \frac{1}{2}\right)}{\left(\kappa_{he} - \frac{3}{2}\right)} + s\delta_{ce}\beta_H\frac{\left(\kappa_{ce} - \frac{1}{2}\right)}{\left(\kappa_{ce} - \frac{3}{2}\right)}\right] \quad (32)$$

$$Q = \left[-\delta_H + \delta_1\beta_{H1}^2 - \delta_2\beta_{H2}^2 + \delta_{he}\beta_{H3}^2\frac{\left(\kappa_{he}^2 - \frac{1}{4}\right)}{(\kappa_{he} - \frac{3}{2})^2} + \delta_{ce}\beta_H^2\frac{\left(\kappa_{ce}^2 - \frac{1}{4}\right)}{(\kappa_{ce} - \frac{3}{2})^2}\right] \quad (33)$$

Taking the derivative of (31) and using equations (28)-(30), the KdVB equation is derived as

$$\frac{\partial \phi^{(1)}}{\partial \tau} + A\phi^{(1)}\frac{\partial \phi^{(1)}}{\partial \xi} + B\frac{\partial^3 \phi^{(1)}}{\partial \xi^3} - C\frac{\partial^2 \phi^{(1)}}{\partial \xi^2} = 0 \quad (34)$$

where the non-linear coefficient $A = \frac{A_1}{A_0}$, $B = \frac{1}{A_0}$ the dispersion coefficient and the dissipation coefficient $C = \frac{A_2}{A_0}$, of

which

$$A_0 = \frac{2}{\lambda^3} \quad (35)$$

$$A_1 = \frac{-3}{\lambda^4} + \frac{3\gamma_1}{\lambda^2} - 2\gamma_2 - s^2 Q \quad (36)$$

and

$$A_2 = \frac{\eta_{d0}}{\lambda^3} \quad (37)$$

Shocks in dusty plasmas have been generally studied using either the Burger's equation [46, 52 – 58] or the Korteweg-deVries-Burgers (KdVB) equation [45, 46, 59 – 64]. Both Manesh et al [45] and Sijo et al [46] had considered five component plasmas; this study can thus be considered as extending and complementing these studies as we have an additional component namely, negatively charged dust grains.

Solution of KdVB equation

The "tanh method" can be used to obtain the shock-like solution of KdVB equation (34) [67 - 69]. We used a transformed co-*ordinate* $\chi = f(\xi - V\tau)$ moving with the shock speed V and employed boundary conditions $\phi^{(1)}$, $\frac{\partial^2 \phi^{(1)}}{\partial \chi^2}$, $\to 0$ as $\chi \to \infty$. For a localized solution, we can write equation (34) as

$$-V\phi^{(1)} + \frac{A}{2}\left|\phi^{(1)}\right|^2 + B\frac{\partial^2 \phi^{(1)}}{\partial \chi^2} - C\frac{\partial \phi^{(1)}}{\partial \chi} = 0 \quad (38)$$

Again using the transformation $\alpha = \tanh\chi$ and assuming a series solution of the form $\phi^{(1)}(\alpha) = \sum_{i=0}^{n}\alpha_i\alpha^i$, the shock solution of KdVB equation is determined as

$$\phi^{(1)} = \frac{3C^2}{25AB}\left[1 - \tanh^2\left[k\left(\xi - V\tau\right)\right]\right] + \frac{V}{A} - \frac{6C^2}{25AB}\tanh\left[k\left(\xi - V\tau\right)\right] \quad (39)$$

where $V = \frac{6C^2}{25B}$ is the shock speed and $k = \frac{\pm C}{10B}$ is the inverse of the shock width.

Results and Discussions

The KdVB equation (34) can be applied to any multi-ion/ dusty plasma environment. However, the parameters relevant to plasma environment of comet Halley are used to plot the figures. The hydrogen ion density was set at $4.95\ cm^{-3}$ with a temperature of $T_H = 8\times10^4 K$; the solar electron temperature $T_{he} = 2\times10^5 K$. The temperature of the colder, cometary electrons was set at $T_{ce} = 2\times10^4 K$. The negatively charged oxygen ion was set at $n_{10} = .05\ cm^{-3}$. The density of the positively charged heavier oxygen ions was $n_{20} = 0.5\ cm^{-3}$ at a temperature of $1.16\times10^4 K$ [41, 42]. The density of dust of negative polarity was set at $n_{d0} = 0.1\ cm^{-3}$ and its equilibrium charge at . Also, $z_{d0} = 50$, $\kappa_{he} = \frac{11}{2}$, $\kappa_{ce} = \frac{7}{2}$ and $z_H = 1$, $z_1 = 4$ and $z_2 = 2$. The values of normalized kinematic dust ion viscosity used was $\eta_{d0} = 0.5$.

(Figure 1) shows a plot of the shock profiles, with and without dust charge variation. The dotted (blue) curve is for $\gamma_1 = 0$, $\gamma_2 = 0$; while the continuous (red) curve is with dust charge variation; obtained for $n_{d0} = 0.1\ cm^{-3}$, $m_d = 200\ a.m.u.$ and $z_{d0} = 50$. The other parameters for the figure are: $T_{he} = 2\times10^5 K$, $T_{ce} = 2\times10^4$, $T_H = 8\times10^4 K$, $T_d = T_1 = T_2 = 1.16\times10^4 K$; the densities are $n_{H0} = 4.95cm^{-3}$, $n_{10} = 0.05cm^{-3}$, $n_{20} = 0.5cm^{-3}$, $n_{d0} = 0.1cm^{-3}$, $n_{he} = n_{ce} = 0.5\ n_e$. From the figure, it is clear that with the inclusion of dust charge variation, the amplitude of the shock wave increases.

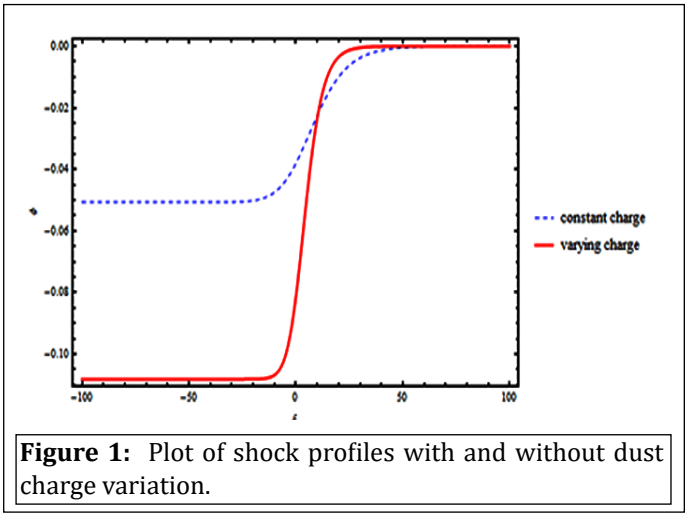

Figure 1: Plot of shock profiles with and without dust charge variation.

In a study related to comet Halley, Tribeche and Bacha [61] concluded that nonlinear damping due to dust charge variation would lead to the formation of shock waves. A similar conclusion was arrived at more recently by Naeem et al [65]. Also the pickup of heavy ions could lead to the formation of shock waves [66]. Also the charge exchange reaction which leads to the formation of negatively charged oxygen ions could also contribute to the formation of shock waves.

(Figure 2) depicts the variation of (a) phase velocity, λ, (b) shock speed, V, and (c) solitary width, W, versus the spectral index kappa, κ_{ce}. Again, the dotted (blue) curves are for the cases where the charges on the dust particles are a constant; the continuous (red) curves depict the other case. The parameters are the same as in figure 1. It is obvious that as the specral index kappa for cometary electron increases, the phase velocity and the shock width increase whereas the shock speed decreases with κ_{ce}. However, with dust charge variation included, the values of phase velocity, and width of the shock wave get reduced but the shock speed increases.

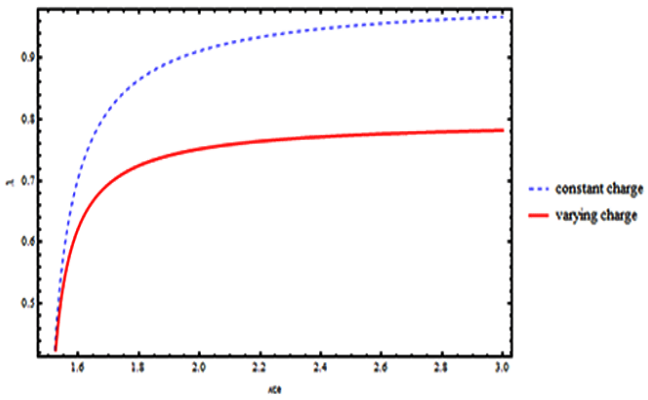

Figure 2a: Variation of phase velocity, λ with spectral index κ_{ce} with and without dust charge variation.

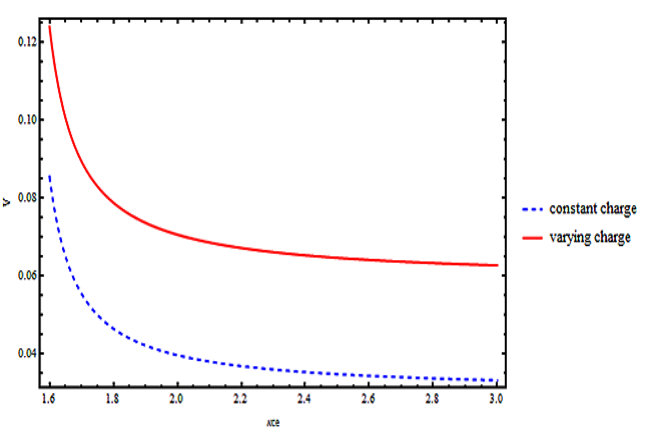

Figure 2b: Variation of shock speed, *V* with spectral index κ_{ce} with and without dust charge variation.

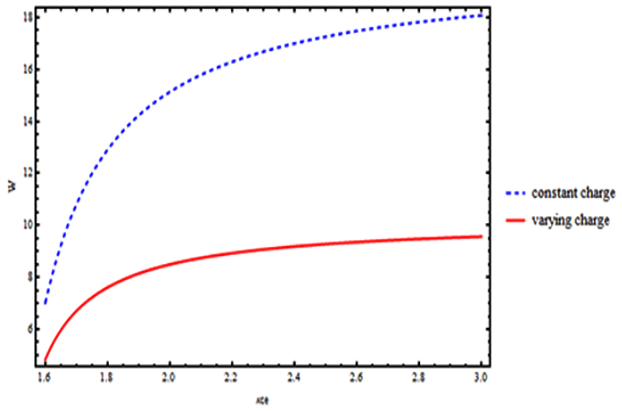

Figure 2c: Variation of the shock width W with spectral index κ_{ce} with and without dust charge variation.

(Figure 3) shows the variation of the phase velocity, λ, versus equilibrium charge number z_{d0}. The dotted (blue) curve depicts the case where the charges on the dust particles are a constant; the continuous (red) curve is for the case where the charge varies. The other parameters are the same as in (figure 1). We find that λ increases with an increase in the equilibrium charge number z_{d0}; also λ is lower when the charges on the dust particles vary.

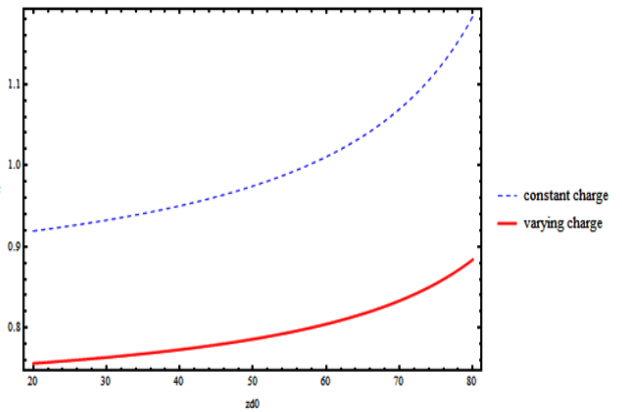

Figure 3: Plot of phase velocity, λ, versus dust charge number, z_{d0}, with and without dust charge variation.

It may be noted that in a study of dust acoustic shock waves in four component plasma of charged mobile dust, kappa distributed electrons, positively charged lighter ions and negatively charged heavier ions; the variation of the phase velocity with κ was similar [40]. Again, in a study of low frequency shocks in a magnetized dusty plasma of negatively charged dust and kappa distributed electrons and ions, the variation of the shock velocity with the spectral index of the ions is similar [62].

Figure 4 depicts the variation of (a) the nonlinear coefficient, A, and (b) the dispersion coefficient, B, with κ_{ce} with and without dust charge variation. Here too, the dotted (blue) curves denote the cases where the charges are on the dust particles are a constant; the continuous (red) curves are for the cases where there is charge variation. The other parameters are the same as in (figure 1). From the figures, it is clear that as the values of κ_{ce} increases, coefficient A and B increases. Also, with dust charge variation included, the value of coefficient A increases whereas B reduces.

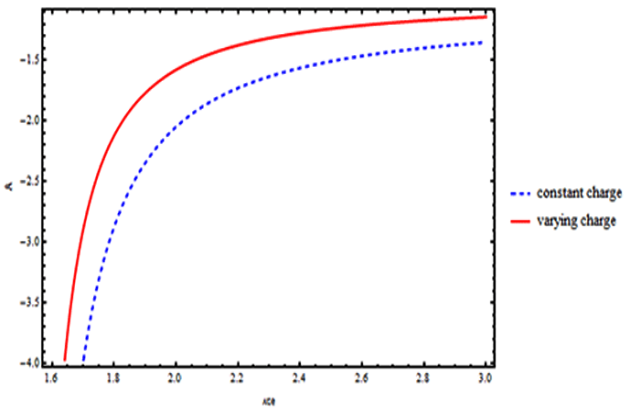

Figure 4a: Variation of the nonlinear coefficient, A with κ_{ce} with and without dust charge variation.

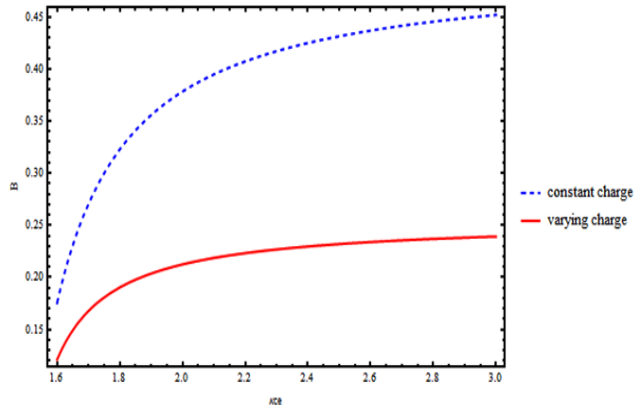

Figure 4b: Variation of the dispersion coefficient, B with κ_{ce} with and without dust charge variation.

(Figure 5) illustrates the variation of the shock amplitudes for different values of the kinematic viscosities of the dust particles with and without dust charge variation. Here too, the dotted (blue) curve represents the case of constant dust charge with $\eta_{d0} = 0.3$ and the dotted (red) curve depicts constant dust charge with $\eta_{d0} = 0.4$. Also the continuous (blue) curve is for the case where the charge varies with $\eta_{d0} = 0.3$ and the continuous (red) curve is for charge variation with $\eta_{d0} = 0.4$. The other parameters are the same as in figure 1. From the plots it is seen that as the kinematic viscosity of the dust particles increase, the amplitude of the shock profile increases. In addition, with the inclusion of dust charge variation, the shock amplitude increases.

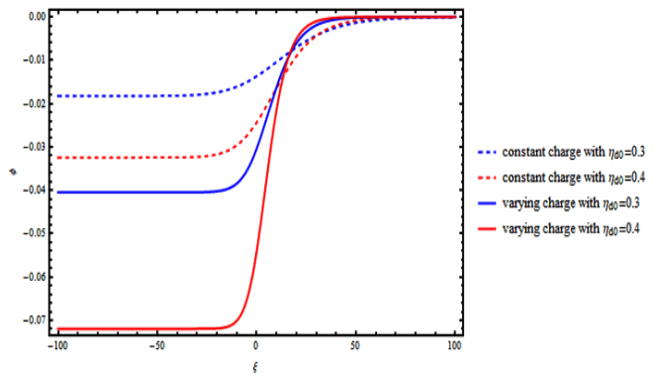

Figure 5: Variation of shock profiles for different values of dust ion kinematic viscosity with and without dust charge variation; the other parameters being the same as in figure 1.

(Figure 6) shows the variation of the shock profiles with (a) negative oxygen ion densities, (b) positive oxygen ion densities and (c) hydrogen ion densities, with and without dust charge variation. The dotted curves represent the cases where the charges on the dust particles are a constant; the continuous curves are for the cases where the charges vary. The blue colour denotes $n_{10} = 0.01\ cm^{-3}$ in figure (a), $n_{20} = 0.04\ cm^{-3}$ in figure (b) and $n_{H0} = 4.4\ cm^{-3}$ in figure (c). The red colour represents $n_{10} = 0.05\ cm^{-3}$ in figure (a), $n_{20} = 0.45\ cm^{-3}$ in figure (b) and $n_{H0} = 4.95\ cm^{-3}$ in figure (c). The other parameters are the same as in figure 1. The shock amplitude decreases with increasing negative oxygen and hydrogen ion densities (in figures 6(a) and 6(c) respectively). However, as the positive oxygen ion densities increase, the shock amplitude increases (figure 6(b)). Further, with inclusion of the variation of dust charge, the shock amplitudes increase as in (figure 1).

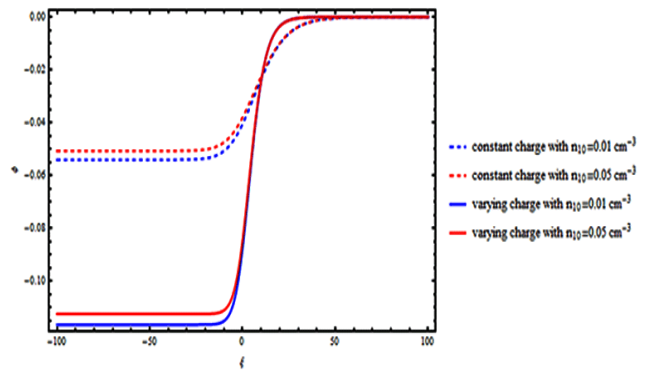

Figure 6a: Variation of shock profile with negative oxygen ion density with and without dust charge variation.

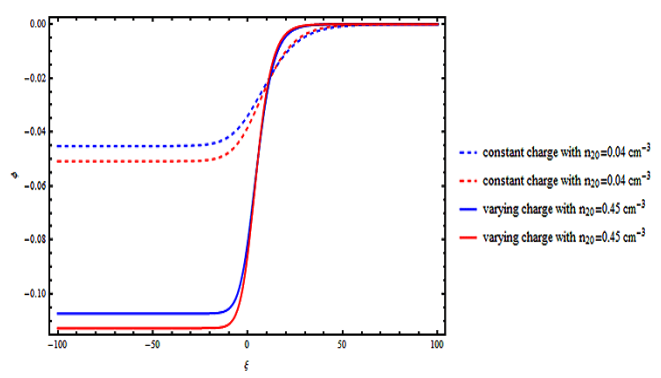

Figure 6b: Variation of shock profile with positive oxygen ion density with and without dust charge variation.

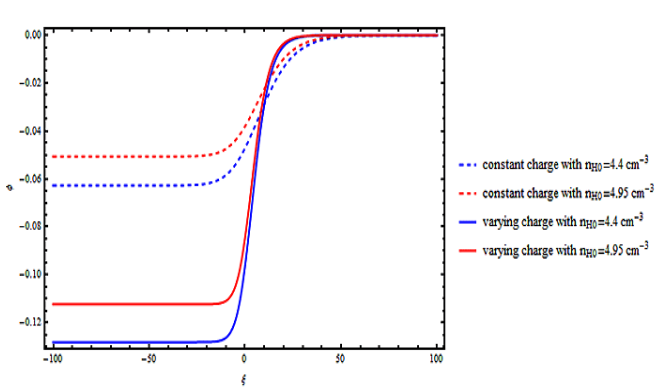

Figure 6c: Variation of shock profile with hydrogen ion density with and without dust charge variation.

(Figure 7) shows the variation of the shock profiles with (a) negative oxygen ion temperatures (b) positive oxygen ion temperatures and (c) hydrogen ion temperatures, with and without dust charge variation. Here too, the dotted curves represent the cases where the charges on the dust particles are a constant; the continuous ones are for the cases where the charges vary. The blue colour denotes $T_i = 1.16\times10^4\,\mathrm{K}$ in figure (a), $T_2 = 1.16\times10^4\,\mathrm{K}$ in figure (b) and $T_H = 8\times10^4\,\mathrm{K}$ in figure (c).The red colour represents $T_i = 5\times1.16\times10^4\,\mathrm{K}$ in figure (a), $T_2 = 5\times1.16\times10^4\,\mathrm{K}$ in figure (b) and $T_H = 5\times8\times10^4\,\mathrm{K}$ in figure (c). The other parameters are the same as in figure 1. The shock amplitude increases with increasing negative oxygen and hydrogen ion temperatures, in figures 7(a) and 7(c) respectively. As the positive oxygen ion temperature increases, the shock amplitude decreases in figure 7(b). Further, with inclusion of the variation of dust charge, the shock amplitude shows the same variation as in figure 1.

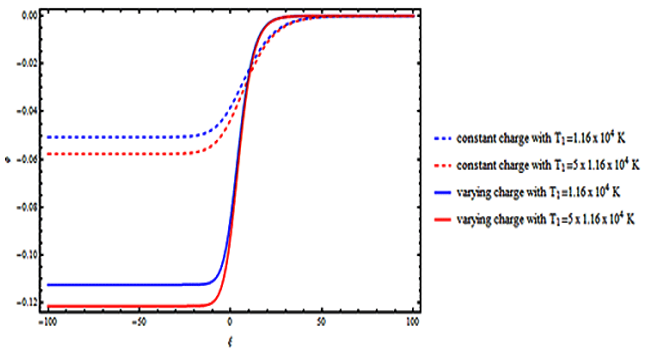

Figure 7a: Variation of shock profile with negative oxygen ion temperature with and without dust charge variation.

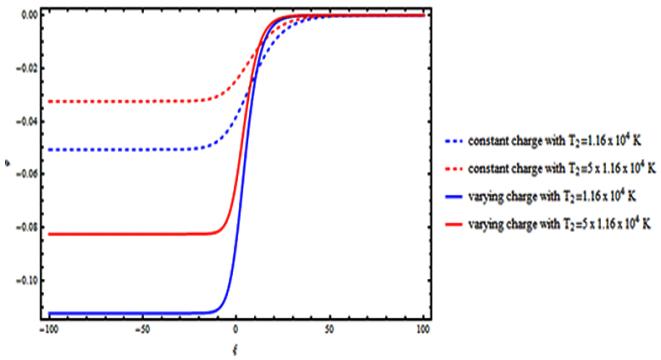

Figure 7b: Variation of shock profile with positive oxygen ion temperature with and without dust charge variation.

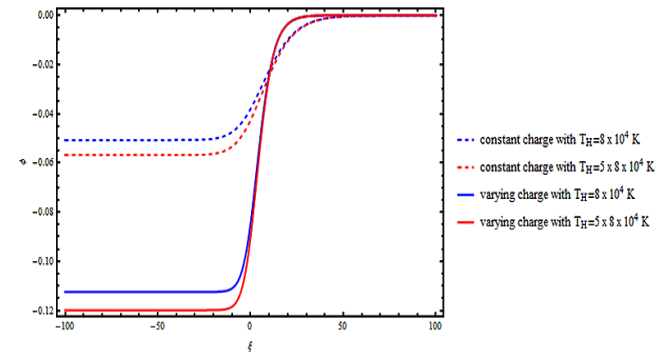

Figure 7c: Variation of shock profile with hydrogen ion temperature with and without dust charge variation.

Conclusion

We have, in this paper, studied dust acoustic shock waves in a six component cometary plasma by deriving the Korteweg-deVries-Burgers (KdVB) equation. The constituents of the plasma include two components of electrons described by kappa distributions with different temperatures and spectral indices, lighter (hydrogen) ions and a pair of oppositely charged, heavier ions (positively and negatively charged oxygen ions), all of them described by Maxwellian distributions with different temperatures. Charge varying negatively charged dust grains is the sixth component.

Shock waves solutions of the KdVB equation, studied for typical parameters of comet Halley, show that the shock amplitudes are consistently larger when charge fluctuations on the dust grains are taken into consideration. The superthermal, second component of electrons affects the phase velocity and the shock velocity as well as it's width. The amplitude of the shock wave is also affected by the densities and temperatures of all the ions: it increases with increasing positively charged oxygen ion densities and decreases with increasing temperatures of these ions. The amplitude, however, decreases with increasing densities and increases with increasing temperatures of the other two types of ions.

Positively and negatively charged nano-grains have been observed at comet 67P / Churyumov – Gerasimenko [70]. Cometary heavy ions (oxygen in our case) picked up by the solar wind produce mass loading resulting in a decrease in the solar wind speed. And these heavy ions play a key role in cometary shocks. Such pick up ions have been observed by Giotto at comet Halley and almost all other comets; such shocks are called "mass loading shocks". An very recently Rosetta was able to cross a newly formed infant bow shock at comet 67P / Churyumov – Gerasimenko. Thus we feel that the results of this paper would contribute to an understanding of shocks observed at comets.

Conflict of Interest

The authors declare that there is no conflict of interest.

References

1. Frank Verheest, Manfred A Hellberg and Ioannis Kourakis. Acoustic solitary waves in dusty and/or multi-ion plasmas with cold, adiabatic, and hot constituents. Physics of Plasmas. 2008;15(11):112309. doi: 10.1063/1.3026716

2. Mannan A, Mamun AA and Shukla PK. Nonplanar solitary waves and double layers in nonthermal electronegative plasma. Physica Scripta. 2012;85(6):065501. doi: 10.1088/0031-8949/85/06/065501

3. Rufai OR, Bharuthram R, Singh SV and Lakhina GS. Obliquely propagating ion-acoustic solitons and supersolitons in four-

component auroral plasmas. Advances in Space Research. 2016;57(3):813-820. doi: 10.1016/j.asr.2015.11.021

4. Maharaj SK, Bharuthram R, Singh SV, Pillay SR and Lakhina GS. Electrostatic solitary waves in a magnetized dusty plasma. Physics of Plasmas. 2008;15(11):113701. doi: 10.1063/1.3028313

5. Shukla PK and Mamun AA. Solitons, shocks and vortices in dusty plasmas. New Journal of Physics. 2003;5(1):1–17. doi: 10.1088/1367-2630/5/1/317

6. Bharuthram R. Arbitrary amplitude double layers in a multi-species electron-positron plasma. Astrophysics and Space Science. 1992;189(2):213–222. doi: 10.1007/BF00643126

7. Mamun AA and Shukla PK. Electrostatic solitary and shock structures in dusty plasmas. Physica Scripta. 2002;T98:107–114. doi: 10.1238/Physica.Topical.098a00107

8. Bharuthram R and Shukla PK. Vortices in non-uniform dusty plasmas. Planetary and Space Science. 1992;40(5):647–654. doi: 10.1016/0032-0633(92)90005-9

9. Vranjes J, Petrovic D and Shukla PK. Low-frequency potential structures in a nonuniform dusty magnetoplasma. Physics Letters A. 2001;278(4):231–238. doi: 10.1016/S0375-9601(00)00749-0

10. Allen JE. Probe theory - The Orbital Motion Approach. Physica Scripta. 1992;45(5):497–503. doi: 10.1088/0031-8949/45/5/013

11. Shukla PK and Mamun AA. Introduction to Dusty Plasma Physics. Plasma Physics and Controlled Fusion. 2002;44(3). doi: 10.1088/0741-3335/44/3/701

12. Mamun AA, Hassan MHA. Effects of dust grain charge fluctuation on an obliquely propagating dust acoustic solitary potential in a magnetized dusty plasma. J. Plasma Physics. 2000;63(2):191–200. doi: 10.1017/S0022377899008028

13. Ghosh S, Bharuthram R, Khan M, Gupta M R. Instability of dust acoustic wave due to nonthermal ions in a charge varying dusty plasma. Phys. Plasmas. 2004;11(7):3602–3609. doi: 10.1063/1.1760584

14. El-Taibany, W F, Wadati M, Sabry R. Nonlinear dust acoustic waves in a nonuniform magnetized complex plasma with nonthermal ions and dust charge variation. Phys. Plasmas. 2007;14(3):2304. doi: 10.1063/1.2646587

15. Murad A, Zakir U, Haque Q. Dust acoustic solitary waves with dust charge fluctuation in superthermal plasma. Braz. J. Phys. 2019;49(1):79–88. doi: 10.1007/s13538-018-0608-2

16. Ghosh S, Sarkar S, Khan M, Gupta M R. Small-amplitude nonlinear dust acoustic waves in a magnetized dusty plasma with charge fluctuation. IEEE Tran.Plasma Sci. 2001;29(3): 409–416. doi: 10.1109/27.928937

17. Benzekka M, Tribeche M. Nonlinear dust acoustic waves in a charge varying complex plasma with nonthermal ions featuring Tsallis distribution. Astrophys. Space Sci. 2012;338(1):63–72. doi: 10.1007/s10509-011-0908-2

18. Zhang L P, Xue J K. Shock wave in magnetized dusty plasmas with dust charging and nonthermal ion effects. Phys. Plasmas. 2005;12(4):042304. doi: 10.1063/1.1868718

19. Popel S I, Gisko A A, Golub A P, Losseva T V, Bingham R, Shukla P K. Shock waves in charge-varying dusty plasmas and the effect of electromagnetic radiation. Phys. Plasmas. 2000;7(6):2410–2416. doi: 10.1063/1.874079

20. Gupta M R, Sarkar S, Ghosh S, Debnath M, Khan M. Effect of nonadiabaticity of dust charge variation on dust acoustic waves: Generation of dust acoustic shock waves. Phys. Rev. E. 2001. doi: 10.1103/PhysRevE.63.046406

21. Misra A P, Chowdhury A R. Dust-acoustic waves in a self-gravitating complex plasma with trapped electrons and nonisothermal ions. Eur. Phys. J. 2006;37:105-113. doi: 10.1140/epjd/e2005-00237-y

22. Tribeche M, Bacha M. Nonlinear dust acoustic waves in a charge varying dusty plasma with suprathermal electrons. Phys. Plasmas. 2010;17(7): 073701-073701.7. doi: 10.1063/1.3449806

23. Duh S S, Shikha B, Mamun A A. Nonlinear dust-ion-acoustic waves in a multi-ion plasma with trapped electrons. Pramana J. Phys. 2011;77(2): 357–368. doi: 10.1007/s12043-011-0102-7

24. Amour R, Tribeche M, Zerguini T H. Nonextensive collisioneless dust-acoustic shock waves in a charge varying dusty plasma. Astrophys. Space Sci. 2012;338(1):, 57–61. doi: 10.1007/s10509-011-0905-5

25. Bacha M, Tribeche, M. Nonextensive dust acoustic waves in a charge varying dusty plasma. Astrophys. Space Sci. 2011;337:253-259. doi: 10.1007/s10509-011-0830-7

26. Shahmansouri M, Tribeche M. Dust acoustic shock waves in suprathermal dusty plasma in the presence of ion streaming with dust charge fluctuations. Astrophys. Space Sci. 343, 251–256. doi: 10.1007/s10509-012-1213-4

27. Hadjaz I, Tribeche M. Alternative dust-ion acoustic waves in a magnetized charge varying dusty plasma with nonthermal electrons having a vortex-like velocity distribution. Astrophys Space Sci. 2014;351:591–598. doi: 10.1007/s10509-014-1872-4

28.El-Shewy, E K, El-Wakil S A, El-Hanbaly A M, Sallah M, Darweesh H F. Effect of nonthermality fraction on dust acoustic growth rate in inhomogeneous viscous dusty plasmas. Astrophys. Space Sci. 2015;356:269-276. doi: 10.1007/s10509-014-2176-4

29.Wang H, Zhang K. Effect of dust size distribution and dust charge fluctuation on dust ion-acoustic shock waves in a multi-ion dusty plasma. Pramana J. Phys. 2016;87:11. doi: 10.1007/s12043-016-1206-x

30.Baluku T K, Hellberg M A. Dust acoustic solitons in plasmas with kappa-distributed electrons and/or ions. Phys. Plasmas. 2008;15(12):123705. doi: 10.1063/1.3042215

31.Mace R L, Amery G, Hellberg, M A. The electron-acoustic mode in a plasma with hot suprathermal and cool Maxwellian electrons. Phys. Plasmas. 1999;6(1):44-49. doi: 10.1063/1.873256

32.Pierrard V, Lazar M. Kappa distributions: Theory and applications in space plasmas. Solar Phys. 2010;267:153-174. doi: 10.1007/s11207-010-9640-2

33.El-Tantawy, S A, El-Bedwehy N A, Khan S, Ali S, Moslem W M. Arbitrary amplitude ion-acoustic solitary waves in superthermal electron-positron-ion magnetoplasma. Astrophys. Space Sci. 2012;342(2): 425-432. doi: 10.1007/s10509-012-1188-1

34.Sultana S, Mamun A A. Linear and nonlinear propagation of ion-acoustic waves in a multi-ion plasma with positrons and two-temperature superthermal electrons. Astrophys. Space Sci. 2014;349(1):229-238. doi: 10.1007/s10509-013-1634-8

35.Vasyliunas V M. A survey of low energy electrons in the evening sector of the magnetosphere with OGO 1 and OGO 3. J. Geophys. Res. 1968;73(9):2839-2884. doi: 10.1029/JA073i009p02839

36.Broiles T W, Livadiotis G, Burc, J L, Chae K, Clark G, Cravens, T.E, et al. Characterizing cometary electrons with kappa distributions. J. Geophys. Res. 2016;121(8):7407–7422. doi: 10.1002/2016JA022972

37.Alinejad H, Tribeche M, Mohammadi M A. Dust ion-acoustic shock waves due to dust charge fluctuation in a superthermal dusty plasma. Phys. Lett. 2011;47(14):4183-4186. doi: 10.1016/j.physleta.2011.10.013

38.Shahmansouri M, Tribeche M. Nonextensive dust acoustic shock structures in complex plasmas. Astrophys Space Sci. 2013;346(1):165-170. doi: 10.1007/s10509-013-1430-5

39.Shah M G, Rahman M M, Hossen M R, Mamun A A. Properties of cylindrical and spherical heavy ion-acoustic solitary and shock structures in a multispecies plasma with superthermal electrons. Plasma Phys. Rep. 2016;42(2):168-176. doi: 10.1134/S1063780X16020069

40.Ferdousi M, Sultana S, Hossena M M, Miah, M R, Mamun A A. Dust-acoustic shock excitations in κ-nonthermal electron depleted dusty plasmas. Eur. Phys. J. D. 2017;71:102. doi: 10.1140/epjd/e2017-80003-4

41.Brinca A L, Tsurutani B T. Unusual characteristics of electromagnetic waves excited by cometary newborn ions with large perpendicular energies. Astron. Astrophys. 1987;187:311–319. doi: 10.1007/978-3-642-82971-0_57

42.Chaizy P, Reme H, Sauvaud J A, d'Uston U, Lin R P, Larson D E. et al. Negative ions in the coma of comet Halley. Nature. 1991;349(6308):393–396. doi: 10.1038/349393a0

43.Ellis T A, Neff J S. Numerical simulation of the emission and motion of neutral and charged dust from P/Halley. Icarus. 1991;91(2):280-296. doi: 10.1016/0019-1035(91)90025-O

44.Chow V W, Mendis D A, Rosenberg M. Role of grain size and particle velocity distribution in secondary electron emission in space plasmas. J. Geophys. Res. 1993;98(11):19065-19076. doi: 10.1029/93JA02014

45.Manesh M, Neethu T W, Neethu J, Sijo S, Sreekala G, Venugopal C. Korteweg-deVries-Burgers (KdVB equation) equation in a five component plasma cometary plasma with kappa described electrons and ions. J. Theor. Appl. Phys. 2016;10(4):280-296. doi: 10.1007/s40094-016-0228-6

46.Sijo S, Anu V, Neethu T W, Manesh M, Sreekala G, Venugopal C. Effect of ion drift on shock waves in an un-magnetized multi-ion plasma. Open Acc. J. Math. Theor. Phy. 2018;1(5):179-184. doi: 10.15406/oajmtp.2018.01.00031

47.Mahmoud A A. Effects of the non-extensive parameter on the propagation of ion acoustic waves in five-component cometary plasma system. Astrophys. Space Sci. 2018;363(1):18. doi: 10.1007/s10509-017-3229-2

48.Pakzad H R. Solitary waves of the Kadomstev-Petviashvili equation in warm dusty plasma with variable dust charge, two temperature ion and nonthermal electron. Chaos, Solitons and Fractals.2009;42(2):874-879. doi: 10.1016/j.chaos.2009.02.016

49.Abid A A, Ali S, Muhammad R. Dust grain surface potential in a non-Maxwellian dusty plasma with negative ions. J. Plasma Phys. 2013;79(6):1117-1121. doi: 10.1017/S0022377813001372

50.El-Taibany W F, Sabry R. Dust-acoustic solitary waves and double layers in a magnetized dusty plasma with nonthermal ions and dust charge variation. Phys. Plasmas. 2005;12(8):082302. doi: 10.1063/1.1985987

51.Washimi H, Taniuti T. Propagation of ion-acoustic solitary waves of small amplitude. Phys. Rev. Lett. 1996;17(19):996-998. doi: 10.1103/PhysRevLett.17.996

52.Mondal G, Chatterjee M. Shock waves in a dusty plasma with positive and negative dust where ions are nonthermal. Z. Naturofirsch. 2010.

53.Ferdousi M, Mamun A A. Electrostatic shock structures in a non-extensive plasma with two distinct temperature electrons. Braz. J. Phys. 2015;45(1):89–94. doi: 10.1007/s13538-014-0285-8

54.Dev A N, Sarma J, Deka M K. Dust acoustic shock waves in arbitrarily charged dusty plasma with low and high temperature nonthermal ions. Can. J. Phys. 2015;93(10)1030 - 1038. doi: 10.1139/cjp-2014-0391

55.Ferdousi M, Miah M R, Sultana S, Mamun A A. Dust acoustic shock waves in an electron depleted, non-extensive dusty plasma. Astrophys. Space Sci. 2015;360:43. doi: 10.1007/s10509-015-2547-5

56.Dev A N, Deka M K, Sarma J, Adhikary N C. Shock wave solution in a hot adiabatic dusty plasma having negative and positive nonthermal ions with trapped electrons. J. Kor. Phys. Soc. 2015;67:339 – 345. doi: 10.3938%2Fjkps.67.339

57.Dev A N. Lower order three-dimensional Burgers equation having non-Maxwellian ions in dusty plasmas. Chin. Phys. B. 2017;26(2):025203. doi: 10.1088/1674-1056/26/2/025203

58.Hossen M M, Nahar L, Alam M S, Sultana S, Mamun A A. Electrostatic shock waves in a nonthermal dusty plasma with oppositely charged dust. High Energy Density Phys. 2017;24:9–14. doi: 10.1016/j.hedp.2017.05.011

59.Pakzad H R, Javidan K. Dust acoustic solitary and shock waves in strongly coupled dusty plasmas with nonthermal ions. Pramana-J. Phys. 2009;73(5):913–926. doi: 10.1007/s00193-011-0331-1

60.Pakzad H R. Dust acoustic shock waves with strongly coupled dusts and superthermal ions. Can. J. Phys. 2011;89(2):193 – 200. doi: 10.1139/P10-110

61.Tribeche M, Bacha M. Dust acoustic shock waves in a charge varying electronegative magnetized dusty plasma with nonthermal ions: Applications to Comets. Phys. Plasmas. 2013;20(10):103704. doi: 10.1063/1.4825240

62.Chahal B S, Ghai Y, Saini N S. Low-frequency shock waves in a magnetized superthermal dusty plasma. J. Theor. Appl. Phys. 2017;11(3):181–189. doi: 10.1007/s40094-017-0260-1

63.Ghai Y, Kaur N, Singh K, Saini N S. Dust acoustic shock waves in magnetized dusty plasma. Plasma Sci. Tech. 2018.

64.Alamri S. On the dissipative propagation in oppositely charged dusty plasmas. Z. Naturofirsch. 2019;7(3):227 – 234. doi: 10.1515/zna-2018-0350

65.Coates A J. Heavy ion effects on cometary shocks. Adv. Space Res. 1995;15(8-9):403-413. doi: 10.1016/0273-1177(94)00125-K

66.Naeem I, Ehsan Z, Mirza A M, Murtaza G, Shocklets in comet Halley plasma. 2020. doi: 10.1063/5.0002521

67.Karimi M. The tanh method for solutions of the nonlinear modified Korteweg de Vries equation. Mathematics Scientific Journal. 2013;9(1):47-54.

68.Malfliet W. Solitary wave solutions of nonlinear wave equations. American J. Phys. 1992;60(7):650-654. doi: 10.1119/1.17120

69.Malfliet W. The tanh method:a tool for solving certain classes of nonlinear evolution and wave equations. J. Comput. Appl. Math. 2004;164(165): 529-541. doi: 10.1016/S0377-0427(03)00645-9

70.Llera K, Burch J L, Goldstein R, Goetz C. Simultaneous observation of negatively and positively charged nano-grains at comet 67P / Churyumov – Gerasimenko Geophys. Res. Lett. 2020. doi: 10.1029/2019GL086147.

71.Neubauer F M, Glassmeier K H, Acuna M H, Mariani F, Musmann G, Ness NF, Coates A J. Giotto magnetic field observations at the out bound quasi-parallel bow shock at comet Halley. Annales Geophysicae. 1990;22(8):463 – 471.

72.Gunell H, Goetz C, Wedlund C S, Lindkvist J, Hamrinm M, Nilsson H, Llera, et al. The infant bow shock: a new frontier at a weak activity comet. 2018. doi: 10.1051/0004-6361/201834225